

Supporting Information

An Fe complex for ^{19}F magnetic resonance-based reversible redox sensing and multicolor imaging

Rahul T. Kadakia,[‡] Raphael T. Ryan,[‡] Daniel J. Cooke, Emily L. Que*

Department of Chemistry, The University of Texas at Austin, 105 E. 24th St Stop A5300, Austin, Texas, 78712, United States

[‡]These Authors contributed equally to this work

emilyque@cm.utexas.edu

Experimental methods	S3
Scheme S1: Synthesis of $\text{Fe}^{\text{II}}\text{DO3ASF}_5$ and $\text{Fe}^{\text{III}}\text{DO3ASF}_5$	S7
Figure S1: Normalized absorbance of $\text{Fe}^{\text{III}}\text{DO3ASF}_5$ with 25 eq. reducing agents	S9
Figure S2: Representative plot of absorbance changes of the reduction of $\text{Fe}^{\text{III}}\text{DO3ASF}_5$ with cysteine over 216 seconds	S9
Figure S3: Zoomed in ^{19}F NMR spectrum of $\text{Fe}^{\text{III}}\text{DO3ASF}_5$	S10
Figure S4: Zoomed in ^{19}F NMR spectrum of $\text{Fe}^{\text{II}}\text{DO3ASF}_5$	S10
Figure S5: Zoomed in ^{19}F NMR spectrum of $\text{Fe}^{\text{III}}\text{DO3ASF}_5$ with 5 eq. cysteine	S11
Figure S6: Oxidation of $\text{Fe}^{\text{II}}\text{DO3ASF}_5$ by H_2O_2 as monitored by UV-vis	S11
Figure S7: Kinetic stability of $\text{Fe}^{\text{III}}\text{DO3ASF}_5$ in the presence of biologically relevant metal ions	S12
Figure S8: ^{19}F NMR spectra of $\text{Fe}^{\text{III}}\text{DO3ASF}_5$ before and after 24 h incubation at 37 °C in 80% human serum and 20% D_2O	S12
Figure S9: ^{19}F NMR spectra of $\text{Fe}^{\text{III}}\text{DO3ASF}_5$ before and after 24 h incubation at 37 °C in 8% human serum, 20% D_2O and 72% 1X Minimum Essential Medium (MEM) containing Earle's salt	S13
Figure S10: pH stability of $\text{Fe}^{\text{III}}\text{DO3ASF}_5$ with and without cysteine	S13
Figure S11: pH stability of $\text{Fe}^{\text{III}}\text{DO3ASF}_5$ with and without cysteine after 7 days	S14
Figure S12: pH stability of $\text{Fe}^{\text{II}}\text{DO3ASF}_5$ before and after two hours	S14

Figure S13: Kinetic stability of $\text{Fe}^{\text{II}}\text{DO3ASF}_5$ in the presence of NaCl	S15
Figure S14: Kinetic stability of $\text{Fe}^{\text{II}}\text{DO3ASF}_5$ in the presence of KCl	S16
Figure S15: Kinetic stability of $\text{Fe}^{\text{II}}\text{DO3ASF}_5$ in the presence of CaCl_2	S17
Figure S16: Kinetic stability of $\text{Fe}^{\text{II}}\text{DO3ASF}_5$ in the presence of MgCl_2	S18
Figure S17: Kinetic stability of $\text{Fe}^{\text{II}}\text{DO3ASF}_5$ in the presence of ZnCl_2	S19
Figure S18: Atmospheric oxidation of 100 μM $\text{Fe}^{\text{II}}\text{DO3ASF}_5$	S19
Figure S19: Chemical structure of CuATSM-F_3 . ⁴	S20
Figure S20: ^{19}F NMR spectra of $\text{Fe}^{\text{III}}\text{DO3ASF}_5$ and CuATSM-F_3 with cysteine and $\text{Na}_2\text{S}_2\text{O}_4$	S20
Figure S21: ^{19}F MRI phantoms of $\text{Fe}^{\text{III}}\text{DO3ASF}_5$ reversibility with cysteine and H_2O_2	S21
Figure S22: ^1H NMR spectrum of DO3ASF_5 in D_2O	S21
Figure S23: ^{13}C NMR spectrum of DO3ASF_5 in $\text{d}_6\text{-DMSO}$	S22
Figure S24: ^{19}F NMR spectrum of DO3ASF_5 in D_2O	S22
Figure S25: ^1H NMR spectrum of $\text{Fe}^{\text{II}}\text{DO3ASF}_5$	S23
Figure S26: FIA ESI ⁺ HRMS of 3	S23
Figure S27: FIA ESI ⁺ HRMS of $^t\text{BuDO3ASF}_5$	S24
Figure S28: FIA ESI ⁺ HRMS of DO3ASF_5	S24
Figure S29: FIA ESI ⁺ HRMS of $\text{Fe}^{\text{III}}\text{DO3ASF}_5$	S25
Figure S30: FIA ESI ⁺ HRMS of $\text{Fe}^{\text{II}}\text{DO3ASF}_5$	S25
References	S26

Experimental Methods

General

Solvents and chemicals were purchased from Sigma-Aldrich, VWR, and Fisher Scientific and used as received. Iron(II) tetrafluoroborate was purchased from Strem Chemicals as a 40–45% aqueous solution and assumed to be 40%. Iron(II) tetrafluoroborate was opened, stored, and used in a Coy anaerobic chamber. All water used in experiments, synthesis and purification was Milli-Q grade water. Human serum (Sigma-Aldrich # H4522) was sourced from human male AB plasma. Deuterated solvents were purchased from Cambridge Isotope Laboratories (Cambridge, MA). All deoxygenated solvents were freeze-pump-thawed unless specified otherwise. Reverse-phase C18 chromatography was performed on a Biotage Isolera One. UV-vis spectra were obtained using an Agilent Technologies Cary 6 UV-vis Spectrophotometer. ^1H , ^{13}C , ^{19}F NMR spectra were measured on either an Agilent MR400 DDR2 NMR with an Agilent OneProbe 5 mm HX with autotuning and Z-gradient (400, 100, 376 MHz, respectively) or a Bruker Avance III HD 500 Mhz with a Prodigy dual 5 mm probe (500, 125, 470 MHz, respectively). ^{19}F T_1 and T_2 relaxation times were measured with an Agilent MR400 DDR2 NMR. The chemical shifts for ^1H and ^{13}C NMR were calibrated to the solvent peak and ^{19}F NMR was calibrated to CFCl_3 ($\delta = 0$ ppm). The determination of ^1H r_1 and r_2 relaxivities was performed on a Pulsar 60 MHz benchtop NMR spectrometer (Oxford Instruments) operating at 37 °C. LC-MS and high-resolution Electrospray Ionization (ESI) mass spectral analyses were performed by the Mass Spectrometry Facility in the Department of Chemistry at UT Austin. Electrochemistry experiments were performed at the Center for Electrochemistry at UT Austin on a CHI 660D electrochemical workstation. All buffers contained double their concentration of KNO_3 to maintain the same ionic strength. ^{19}F MR images were obtained in the Biomedical Imaging Center at UT Austin using a Bruker BioSpin Pharmascan 70/16 magnet (Karlsruhe, Germany) with a single loop 8 mm surface coil (282.2 MHz) from Doty Scientific.

Cyclic voltammetry

Cyclic voltammetry (CV) measurements for a 1 mM solution of $\text{Fe}^{\text{III}}\text{DO3ASF}_5$ in deoxygenated 0.1 M KCl adjusted to pH 5 with deoxygenated 1 M HCl were recorded using scan speeds ranging from 50 – 400 mV/s. A three-electrode cell was used, including a glassy carbon working electrode, a Ag/AgCl reference electrode containing 3 M KCl, and a platinum wire as auxiliary electrode.

Molar absorptivity

To measure the molar absorptivity, a 25 mM DMSO stock solution of $\text{Fe}^{\text{III}}\text{DO3ASF}_5$ was added to Milli-Q grade water until a final concentration of 100 μM $\text{Fe}^{\text{III}}\text{DO3ASF}_5$ in 5 mM HEPES (pH 7.4), 10 mM KNO_3 (0.4% DMSO) was obtained. Serial dilutions (20 μM – 80 μM) of the 100 μM $\text{Fe}^{\text{III}}\text{DO3ASF}_5$ were made using 0.4% DMSO in 5 mM HEPES (pH 7.4), 10 mM KNO_3 . The absorbance at 310 nm of each solution was determined and plotted against the respective concentration to obtain the molar absorptivity $\epsilon = 3280 \text{ M}^{-1}\text{cm}^{-1}$ with an R^2 value of 0.9994.

Iron content measurements

Solution-mode ICP-MS analysis was performed on an Agilent 7500ce. 10 μL Fe complex solution (25 mg/mL) was diluted to 1.00 mL with TraceMetal grade nitric acid (Fisher Scientific, 67 - 70%, Fe < 1 ppb). The complexes were digested for 24 h and then diluted to 2% v/v HNO_3 for ICP-MS

analysis. A calibration curve was prepared for Fe concentration in the range of 1 – 1000 ppb. Sc was used as internal standard for analysis.

Reduction of Fe^{III}DO3ASF₅ with cysteine, dithiothreitol, and glutathione

All solvents and solutions used for this experiment were deoxygenated and experiments were performed in an air-free cuvette. A 25 mM DMSO stock solution of Fe^{III}DO3ASF₅ was added to Milli-Q grade water until a final concentration of 25 μM Fe^{III}DO3ASF₅ in 5 mM HEPES (pH 7.4), 10 mM KNO₃ (0.1% DMSO) was obtained. The UV-vis absorption spectrum was scanned. Additional samples were prepared such that the final concentrations of all components were 25 μM Fe^{III}DO3ASF₅, 125 μM reducing agent (cysteine, dithiothreitol (DTT), or glutathione (GSH)), and 5 mM HEPES (pH 7.4), 10 mM KNO₃ (0.1% DMSO). Samples were scanned every five minutes until three similar absorption spectra were obtained. The experiment was repeated with a final concentration of 625 μM reducing agent. To determine if one equivalent of cysteine was sufficient to reduce Fe^{III}DO3ASF₅, a 100 μM Fe^{III}DO3ASF₅ was prepared in 5 mM HEPES (0.8% DMSO) with and without 100 μM cysteine and scanned every five minutes until three similar absorption spectra were obtained.

Kinetic evaluation of the reduction of Fe^{III}DO3ASF₅ with cysteine and oxidation with H₂O₂

All solvents and solutions used for this experiment were deoxygenated. The kinetic experiments were performed under pseudo first-order conditions with 25 μM of Fe^{III}DO3ASF₅ and excess cysteine (150–350 μM). The reactions were conducted in 5 mM HEPES (pH 7.4), 10 mM KNO₃ at room temperature. Cysteine stocks were freshly made in acidic water (~ pH 5.4) for each measurement and used within 5 minutes to slow possible formation of disulfide bonds. The absorbance of Fe^{III}DO3ASF₅ was monitored by UV-vis every 6 seconds between 220–550 nm for 10 minutes. The natural log of the absorbance change at 310 nm was plotted against time to obtain the pseudo first-order rate constant from the slope of a linear regression. The pseudo second-order constant was obtained by plotting the pseudo first-order rate constants as a function of cysteine concentration.

Oxidation with hydrogen peroxide (H₂O₂) was evaluated in degassed 5 mM HEPES (pH 7.4), 10 mM KNO₃ at room temperature. Solutions of cysteine and H₂O₂ were freshly made before each measurement. 25 μM solutions of Fe^{III}DO3ASF₅ were prepared in an anaerobic chamber in air-free cuvettes and their absorbance measured. 25 μM of cysteine was added by syringe via the septa and absorbance measurements were taken until three similar readings were obtained. Subsequently, H₂O₂ (1–10 eq.) was added and measurements were recorded every 6 seconds until the absorbance stabilized.

Atmospheric oxidation of Fe^{II}DO3ASF₅ monitored by UV-vis

This experiment was setup in an anaerobic chamber using degassed solutions and solvents. The aerobic oxidation Fe^{II}DO3ASF₅ was measured using UV-vis spectroscopy. A 25 mM aqueous stock of Fe^{II}DO3ASF₅ was diluted into 5 mM HEPES (pH 7.4), 10 mM KNO₃ to give 100 μM Fe^{II}DO3ASF₅. An absorption spectrum was measured, and the air-free cuvette was opened to atmospheric air. Absorption spectra were measured at regular intervals over 18 h and the changes plotted.

Kinetic stability of Fe^{II}DO3ASF₅ and Fe^{III}DO3ASF₅ in the presence of biologically relevant metal ions

Fe^{II}DO3ASF₅: This experiment was performed in an anaerobic chamber using degassed solutions and solvents. A 25 mM D₂O stock of Fe^{II}DO3ASF₅, was diluted into 50 mM HEPES buffer (pH 7.4) to make five 1.2 mM solutions containing 100 mM NaCl, 100 mM KCl, 10 mM CaCl₂, 10 mM MgCl₂, or 100 μM ZnCl₂. Half of each sample was diluted with D₂O to give 20% D₂O and 1 mM Fe^{II}DO3ASF₅ solution and ¹⁹F NMR spectra were obtained for each mixture. The remaining half of the five mixtures were incubated at 37 °C for 24 h and their ¹⁹F NMR spectra were recorded after diluting with D₂O (20% D₂O total).

Fe^{III}DO3ASF₅: A 25 mM DMSO stock of Fe^{III}DO3ASF₅ was used to prepare 5 samples such that the final concentrations of all species were 100 μM Fe^{III}DO3ASF₅ in 43.75 mM HEPES (0.4% DMSO) with their respective ions: 100 mM NaCl, 100 mM KCl, 10 mM CaCl₂, 10 mM MgCl₂, or 100 μM ZnCl₂. Their UV-vis absorption was taken, and all samples were incubated at 37 °C for 24 hours and their absorbances were remeasured.

Human serum stability of Fe^{III}DO3ASF₅

A 25 mM DMSO stock of Fe^{III}DO3ASF₅ was directly diluted into human serum with 20% D₂O or into 8% human serum, 72% 1X Minimum Essential Medium (MEM) containing Earle's salts, and 20% D₂O to make 1 mM solutions. An initial ¹⁹F NMR spectrum was measured for each sample and the mixtures were incubated for 24 h at 37 °C. A final measurement was performed upon completion of the incubation stage.

Reduction and pH stability studies of Fe^{II/III} DO3ASF₅ monitored by ¹⁹F NMR

All solvents and solutions used for this experiment were deoxygenated. Two solutions were prepared: the first contained 1 mM Fe^{III}DO3ASF₅ in 25 mM HEPES (pH 7.4) with 20% DMSO and 20% D₂O and the second contained the same as the first solution with 5 mM (five equivalents) of cysteine added. Two additional samples were prepared in 25 mM MES buffer (pH 6) for acidic stability studies. All NMR tubes were scanned after preparation and seven days later. To test the pH stability of Fe^{II}DO3ASF₅, two samples were made: the first contained 1 mM Fe^{II}DO3ASF₅ in 5 mM HEPES (pH 7.4) with 10% DMSO and 10% D₂O and the second contained the same as the first solution except with 5 mM MES (pH 6) as the buffer. Both NMR samples were scanned upon preparation and two hours later.

¹⁹F NMR relaxation time measurements

All solvents and solutions used for this experiment were deoxygenated and the samples were prepared in an anaerobic chamber. The ¹⁹F *T*₁ and *T*₂ values of 1 mM solutions of the synthesized and the *in situ* generated Fe^{II}DO3ASF₅ complexes were measured using a 400 MHz NMR spectrometer. A DMSO stock of Fe^{III}DO3ASF₅ and a D₂O stock Fe^{II}DO3ASF₅ were used to make samples. The *in situ* reduced complex was generated with five equivalents of freshly prepared dithiothreitol (DTT, dissolved in water) using a 25 mM stock of Fe^{III}DO3ASF₅. Each sample contained 20% D₂O, 4% DMSO in 5 mM HEPES (pH 7.4). ¹⁹F *T*₁ and *T*₂ were measured at 376 MHz using inversion recovery and Carr-Purcell-Meiboom-Gill (CPMG) pulse sequences, respectively.

Determination of ^1H r_1 and r_2 relaxivities of $\text{Fe}^{\text{III}}\text{DO3ASF}_5$

A DMSO stock of $\text{Fe}^{\text{III}}\text{DO3ASF}_5$ was diluted into PBS (1X, pH 7.4) at 0–1 mM concentrations and measurements were made at 37 °C. ^1H T_1 and T_2 relaxation times were measured at 60 MHz using inversion recovery and CPMG pulse sequences, respectively.

Redox reversibility experiments

All solvents and solutions used for this experiment were deoxygenated and UV-vis experiments were performed in an air-free cuvette. Five samples were prepared such that they all contained 0.5 mM $\text{Fe}^{\text{III}}\text{DO3ASF}_5$ in 5 mM HEPES (pH 7.4), 10 mM KNO_3 with 2% DMSO and 10% D_2O . ^{19}F NMR (32 scans) and UV-vis (1:5 dilution with Milli-Q grade water to obtain 0.1 mM $\text{Fe}^{\text{III}}\text{DO3ASF}_5$) spectra were obtained. Next, the four remaining samples were reduced with 1 equivalent cysteine and one of the samples was subjected to ^{19}F NMR and UV-vis after complete reduction. Then, the three remaining samples were oxidized with 10 eq H_2O_2 and one of the samples was subjected to ^{19}F NMR and UV-vis after complete oxidation. After that, the two remaining samples were reduced with 12.5 eq cysteine and one of the samples was subjected to ^{19}F NMR and UV-vis after complete reduction. Finally, the last sample was oxidized with 50 eq H_2O_2 and was subjected to ^{19}F NMR and UV-vis after complete oxidation. All UV-vis samples were diluted further to confirm their mass via LC-MS.

Magnetic moment determination

The effective magnetic moment was determined based on a modified Evans' method.^{1, 2} Two solutions were prepared: the first contained 5 mM $\text{Fe}^{\text{III}}\text{DO3ASF}_5$ in 5% $^1\text{BuOH}$ in d_6 -DMSO, which was placed inside of a coaxial NMR tube insert, and the second contained 5% $^1\text{BuOH}$ in d_6 -DMSO, which was placed inside of the NMR tube. Then, the NMR tube containing the coaxial insert was subjected to a 400 MHz NMR. The change in chemical shift between the two $^1\text{BuOH}$ peaks was obtained and used to determine the effective magnetic moment (μ_{eff}):

$$\chi_g = \frac{(-3\Delta f)}{4\pi f m} + \chi_0 + \frac{\chi_0(d_0 - d_s)}{m} \quad (\text{Eq. 1})$$

$$\mu_{eff} = 2.84(\chi_m T)^{1/2} \quad (\text{Eq. 2})$$

χ_g is the mass susceptibility of the solute, χ_0 is the mass susceptibility of the solvent, χ_m is the molar susceptibility, Δf is the frequency shift of the reference in Hz, f is the spectrometer frequency in Hz, m is the mass of the substance per mL of solution, d_0 and d_s are the densities of the solvent and solution, and T is the temperature in K. The same procedure was used to measure the magnetic moment of $\text{Fe}^{\text{II}}\text{DO3ASF}_5$ with the use of D_2O instead of DMSO-d_6 .

^{19}F MR imaging

Four samples were prepared at a final volume of 250 μL inside a 300 μL Eppendorf tube using deoxygenated solvents in an anaerobic chamber. The first two samples contained 3 mM $\text{Fe}^{\text{III}}\text{DO3ASF}_5$ in 1:1 DMSO:HEPES (pH 7.4, 25 mM final concentration) with and without one equivalent cysteine. The second two samples contained 5 mM CuATSM-F_3 in 3:1 DMSO:HEPES (pH 7.4, 25 mM final concentration) with and without one equivalent of sodium dithionite. All four samples were imaged using both the CF_3 (282.550 MHz) and the SF_5 (282.588 MHz) frequency. To obtain the reoxidized sample, the 3 mM $\text{Fe}^{\text{III}}\text{DO3ASF}_5$ tube was opened to atmospheric air and 20 equivalents H_2O_2 was added and reimaged.

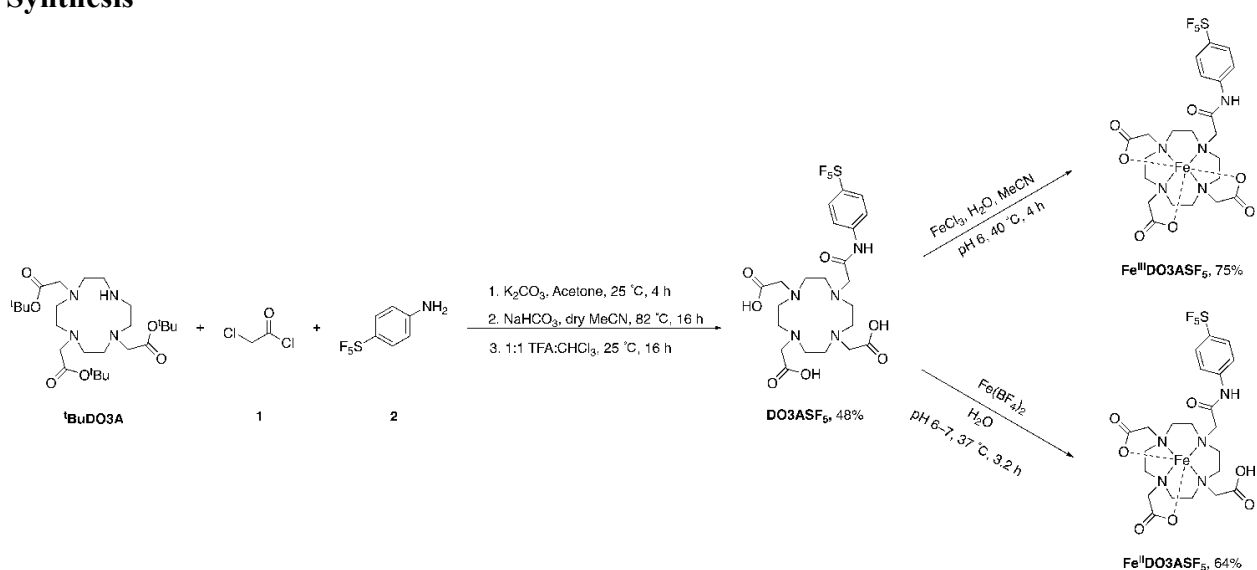
^{19}F MR images were obtained using a single loop 8 mm surface coil (282.2 MHz) from Doty Scientific. The coil was referenced to the CF_3 frequency using pure fomblin and to the SF_5

frequency using 10 M 4-(pentafluorosulfanyl)aniline (compound **2**) in DMSO. After referencing, a single pulse of the reduced sample was obtained, and the frequency (in MHz) was corrected to match the complex. The following parameters were used during imaging:

CF₃: Rapid acquisition with relaxation enhancement (RARE) pulse sequence, 1500 mms repetition time, 46 ms echo time, 300 averages, 7.667 ms echo spacing, rare factor 16, 90° flip angle, 10 mm slice thickness, 32x32 matrix, and a 40x40 mm² field of view. The total acquisition time was 15 minutes.

SF₅: RARE pulse sequence, 300 ms repetition time, 46 ms echo time, 1500 averages, 7.667 ms echo spacing, rare factor 16, 20° flip angle, 10 mm slice thickness, 32x32 matrix, and a 40x40 mm² field of view. The total acquisition time was 15 minutes.

Synthesis

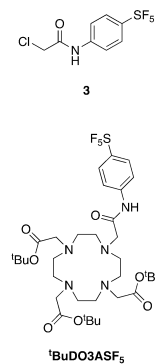


Scheme S1 – Synthesis of Fe^{II}DO3ASF₅ and Fe^{III}DO3ASF₅. Ligand ^tBuDO3A was synthesized following a literature procedure.³

DO3ASF₅

K₂CO₃ (266.7 mg, 1.93 mmol, 4 eq) and **2** (211.6 mg, 0.966 mmol, 2 eq) were added to 20 mL acetone. Then, a solution containing **1** (92.3 μL, 1.16 mmol, 2.4 eq) in 10 mL acetone was added dropwise to the first mixture. The reaction was stirred at room temperature for four hours before quenching the reaction with 30 mL H₂O. The desired intermediate product (**3**) was extracted using ethyl acetate (3 x 30 mL), washed with brine (3 x 30 mL), dried over Na₂SO₄, and transferred to a flame-dried flask before evaporating to dryness. Then, ^tBuDO3A³ (250 mg, 0.486 mmol, 1 eq) and NaHCO₃ (81.2 mg, 0.967 mmol, 2 eq) were added to the flask, sealed, and the air was replaced with N₂ before adding 25 mL dry MeCN. The reaction was heated to 82 °C and stirred overnight. The reaction was cooled, filtered, and subjected to silica gel chromatography. The crude mixture was adsorbed onto silica gel and dry loaded onto the column before eluting with 100% DCM then 30:1 DCM:MeOH to remove less polar impurities. Finally, to isolate the desired ^tBu protected intermediate (^tBuDO3ASF₅), the column was eluted with 15:1 DCM:MeOH. Then, ^tBuDO3ASF₅ was transferred to a scintillation vial and 4 mL of a 1:1

TFA:CHCl₃ solution was added to the vial and allowed to react overnight at room temperature. The next morning, the solvent was removed, and the dried crude product was suspended in 1 mL H₂O and directly injected into a C18 reverse phase chromatography column. The desired product was purified using a 5% MeCN/95% H₂O/0.1% formic acid to 100% MeCN /0.1% formic acid gradient (12 minute LC/MS R_t: 3.9 min). The product was isolated using 62% MeCN/38% H₂O/0.1% formic acid. The product was lyophilized to remove solvents to obtain 180 mg **DO3ASF₅** (48%) as a white solid. ¹H NMR (400 MHz; D₂O) δ 7.82 (d, *J* = 9.2 Hz, 2H), 7.64 (d, *J* = 8.9 Hz, 2H), 3.83 (s, 4H), 3.69 (s, 2H), 3.55 (s, 4H), 3.45 (t, *J* = 4.9 Hz, 6H), 3.21–3.01 (m, 8H). ¹³C NMR (125 MHz, d₆-DMSO, 25 °C): δ 171.18, 170.09, 169.61, 142.25, 126.39, 119.29, 59.61, 55.55, 54.73, 51.49, 50.96, 49.55, 49.35. ¹⁹F NMR (376 MHz; D₂O): δ 85.67 (quintet, *J* = 149.5, 1F), 63.16 (d, *J* = 148.8, 4F). HR ESI-MS (ESI⁺, MeOH): calculated for [C₂₂H₃₂F₅N₅O₇S + H]⁺ 606.2015, found 606.2015.



Synthesis of Fe^{III}DO3ASF₅

DO3ASF₅ (30 mg, 0.0495 mmol, 1 eq) was dissolved in 2 mL H₂O. Then, FeCl₃ (14.7 mg, 0.0906 mmol, 1.8 eq) and enough MeCN was added to fully dissolve all compounds. If necessary, the pH was adjusted to between 5–6 with 1 M NaOH. The mixture was allowed to react at 40 °C for 2 hours, then another 1.1 eq of FeCl₃ (7.4 mg, 0.0456 mmol) was added and reacted until all the ligand was metalated (another two hours; tracked via LC/MS). Upon completion, the solution was directly injected into a C18 reverse phase chromatography column. The desired product was purified using a 5% MeCN/95% H₂O/0.1% formic acid to 100% MeCN/0.1% formic acid gradient (12 minute LC/MS R_t: 4.7 min). The product was isolated using 40% MeCN/60% H₂O/0.1% formic acid. The product was lyophilized to obtain 24.5 mg **Fe^{III}DO3ASF₅** (75%) as a yellow solid. HR ESI-MS (ESI⁺, MeOH): calculated for [C₂₂H₂₉F₅FeN₅O₇S + Na]⁺ 681.0950, found 681.0964. Iron content measured with ICP-MS calcd for 8.50% iron: found: 8.54 ± 0.09%

Synthesis of Fe^{II}DO3ASF₅

Synthesis of **Fe^{II}DO3ASF₅** was carried out in an anaerobic chamber with deoxygenated solvents and solutions. Purification was done quickly under air with highly nitrogen sparged solvents used to prime and elute the product column. The pH of the reaction was monitored with pH paper. A scintillation vial was charged with **DO3ASF₅** (0.0183 g, 0.0302 mmol, 1 eq), a stir bar, and 1 mL of H₂O. The pH of the solution was raised to 6–7 with 1 M NaOH and heated with strong stirring to 37 °C in a water bath. Aqueous Fe(BF₄)₂ (36.0 μL of ~40%, ~0.0604 mmol, ~2 eq) was slowly added to the warm solution. The resulting yellow mixture was heated at 37 °C for 30 min. Subsequently, the pH of the warmed reaction mixture was slowly raised over 40 min to 6–7 with 1 M NaOH. The reaction was allowed to continue at this pH at 37 °C for 90 min. Excess iron was precipitated by raising the pH to ~8 with 1 M NaOH and allowing the suspension to stir at 37 °C for 30 min. The mixture was loaded onto the top of a Biotage® Sfär C18 Duo column frit and pushed into the column bed with a nitrogen-filled syringe. The product was eluted with a gradient of water and methanol. Fractions collected were stored under nitrogen, quickly frozen and lyophilized to give 12.8 mg **Fe^{II}DO3ASF₅** as a white solid (64%). ¹⁹F-NMR (376 MHz; D₂O): δ 63.43 (d, *J* = 148.7 Hz). ¹H NMR see Fig. S25. HR ESI-MS (ESI⁺, MeOH): calculated for [C₂₂H₃₀F₅FeN₅O₇S + H]⁺ 660.1209, found 660.1200. Iron content measured with ICP-MS calcd for 8.49% iron: found: 8.51 ± 0.02%

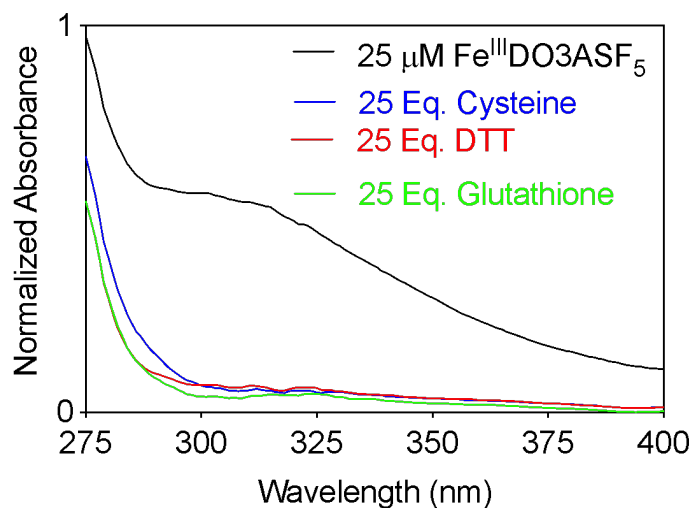


Figure S1 – Normalized absorbance of 25 μM Fe^{III}DO₃ASF₅ in deoxygenated 5 mM HEPES (pH 7.4), 10 mM KNO₃ (0.1% DMSO) with 25 equivalents of reducing agents after five minutes.

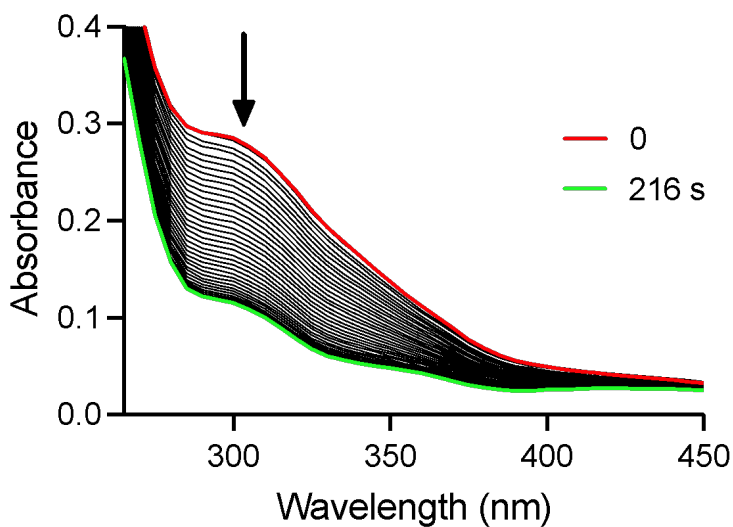


Figure S2 – Representative plot of absorbance changes of the reduction of Fe^{III}DO₃ASF₅ (25 μM) with cysteine (150 μM) over 0 (red) to 216 seconds (green). Reaction performed in 5 mM HEPES (pH 7.4), 10 mM KNO₃.

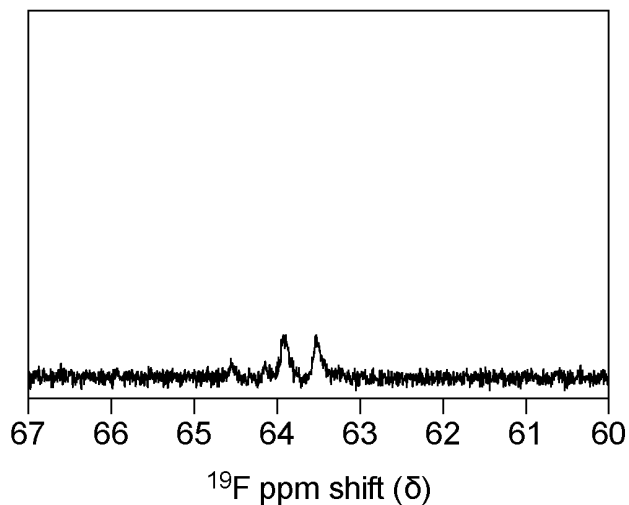


Figure S3 – ^{19}F NMR spectrum of 1 mM $\text{Fe}^{\text{III}}\text{DO3ASF}_5$ in deoxygenated 25 mM HEPES (pH 7.4), 50 mM KNO_3 with 20% DMSO and 20% D_2O zoomed in between +60 and +67 ppm to show broadened doublet. The quintet was not visible.

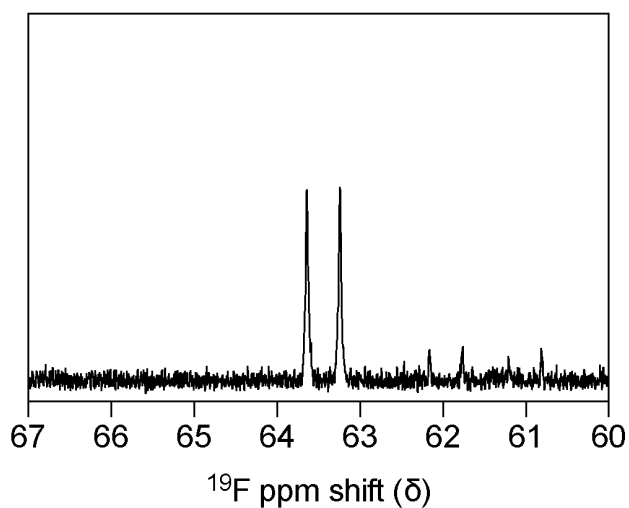


Figure S4 – ^{19}F NMR spectrum of 1 mM $\text{Fe}^{\text{II}}\text{DO3ASF}_5$ in deoxygenated 5 mM HEPES (pH 7.4), 10 mM KNO_3 with 10% DMSO and 10% D_2O zoomed in between +60 and +67 ppm. The quintet was not visible.

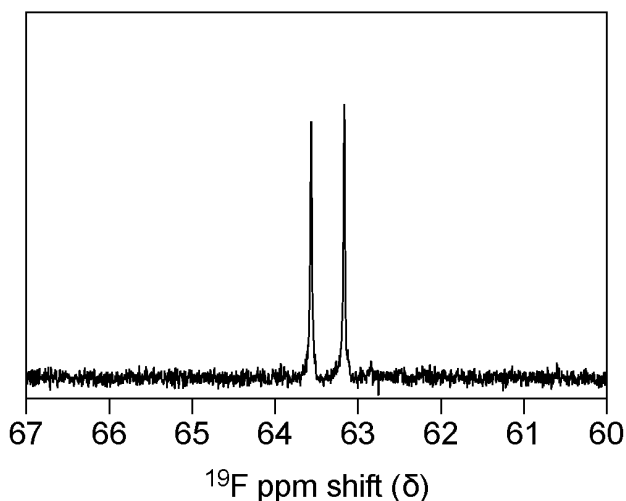


Figure S5 – ^{19}F NMR spectrum of 1 mM $\text{Fe}^{\text{III}}\text{DO3ASF}_5$ in deoxygenated 25 mM HEPES (pH 7.4) with five equivalents cysteine, 20% DMSO, and 20% D_2O zoomed in between +60 and +67 ppm to show broadened doublet. The quintet was not visible.

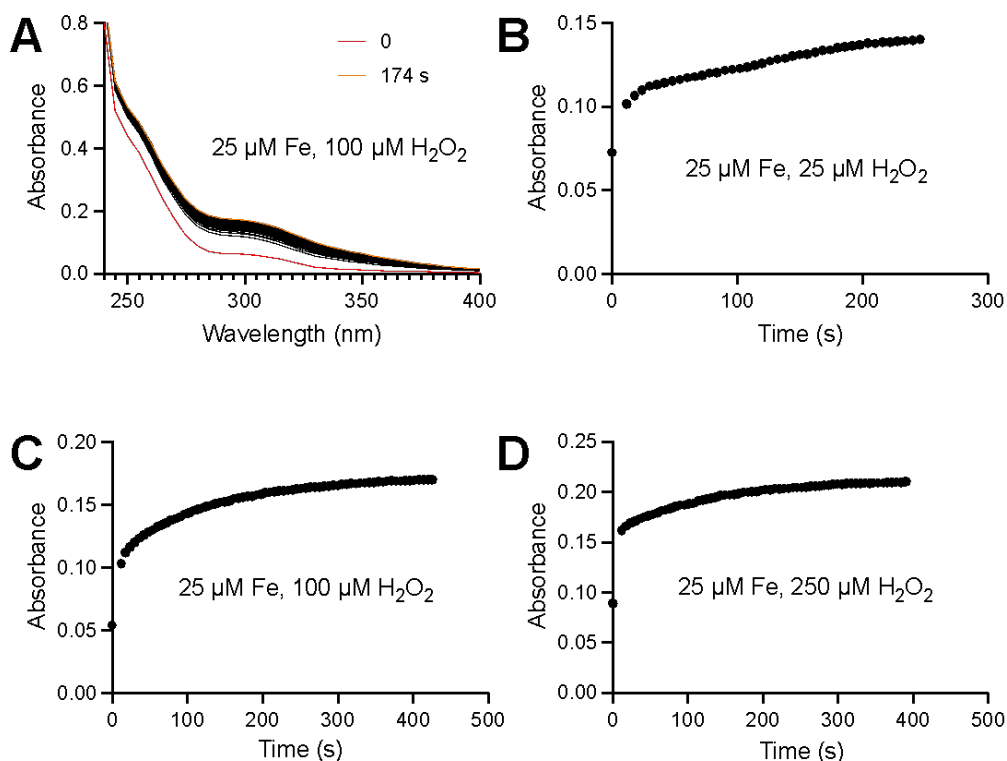


Figure S6 – Oxidation of $\text{Fe}^{\text{II}}\text{DO3ASF}_5$ by H_2O_2 as monitored by UV-vis. A) Representative plot of absorbance changes for the reaction between 25 μM $\text{Fe}^{\text{II}}\text{DO3ASF}_5$ with 100 μM H_2O_2 . Absorbance of solution of 25 μM $\text{Fe}^{\text{II}}\text{DO3ASF}_5$ at 310 nm in the presence of various equivalents of H_2O_2 B) 1 equiv C) 4 equiv D) 10 equiv. All reactions performed in 5 mM HEPES (pH 7.4), 10 mM KNO_3 .

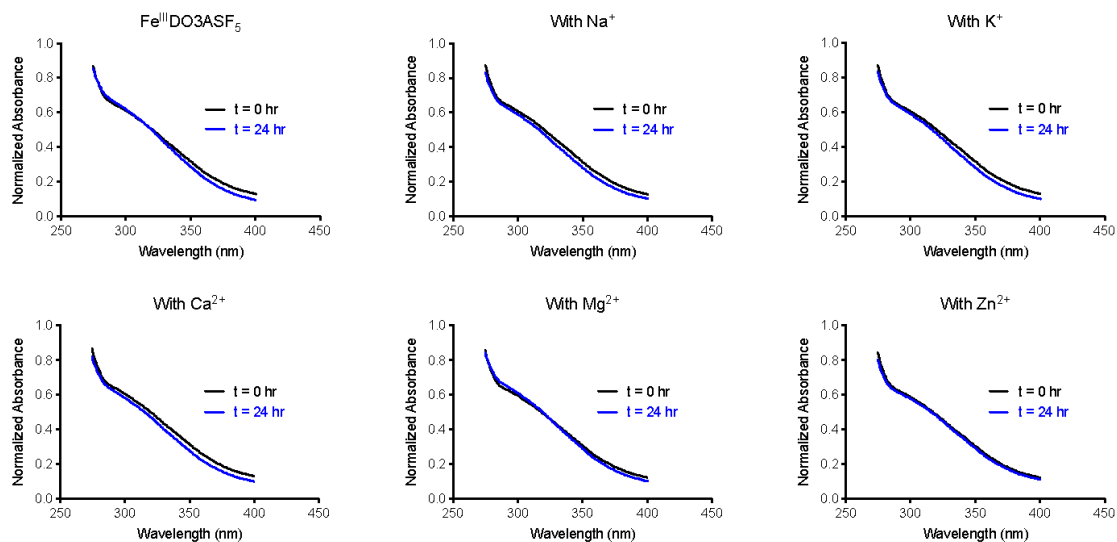


Figure S7 – Kinetic stability of $\text{Fe}^{\text{III}}\text{DO3ASF}_5$ in the presence of biologically relevant metal ions. UV-vis spectra of $\text{Fe}^{\text{III}}\text{DO3ASF}_5$ (100 μM) in 43.75 mM HEPES in the presence of 100 mM NaCl, 100 mM KCl, 10 mM CaCl_2 , 10 mM MgCl_2 , or 100 μM ZnCl_2 before (black) and after (blue) incubation at 37 $^\circ\text{C}$ for 24 h.

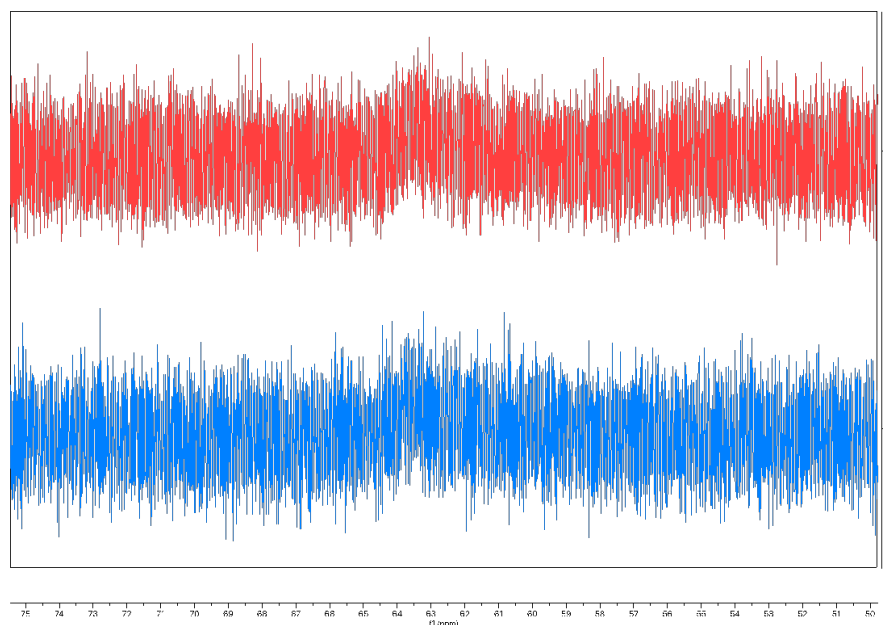


Figure S8 – ^{19}F NMR spectra of $\text{Fe}^{\text{III}}\text{DO3ASF}_5$ (1 mM) before (bottom, blue) and after (top, red) 24 h incubation at 37 $^\circ\text{C}$ in 80% human serum and 20% D_2O .

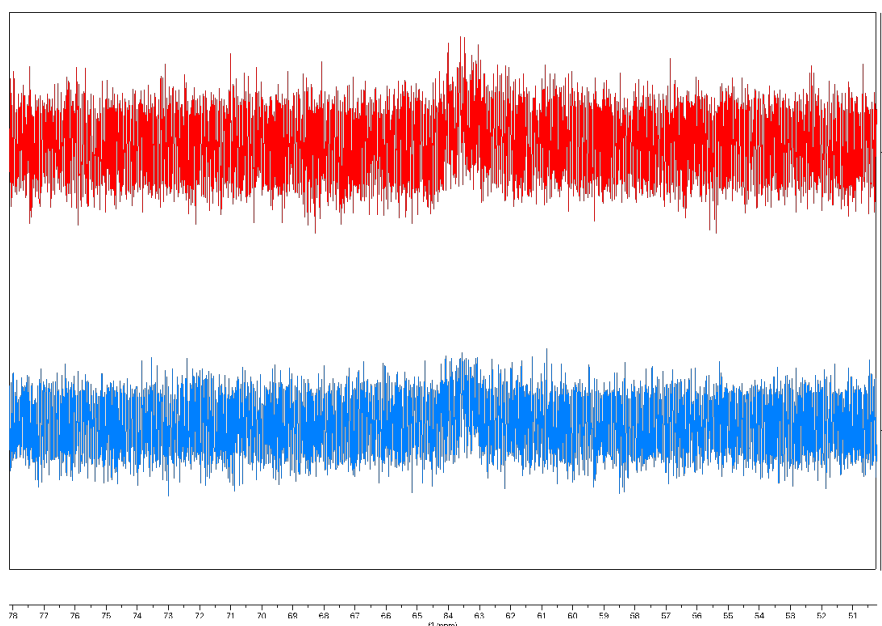


Figure S9 – ^{19}F NMR spectra of $\text{Fe}^{\text{III}}\text{DO}_3\text{ASF}_5$ (1 mM) before (bottom, blue) and after (top, red) 24 h incubation at 37 °C in 8% human serum, 20% D_2O and 72% 1X Minimum Essential Medium (MEM) containing Earle's salts.

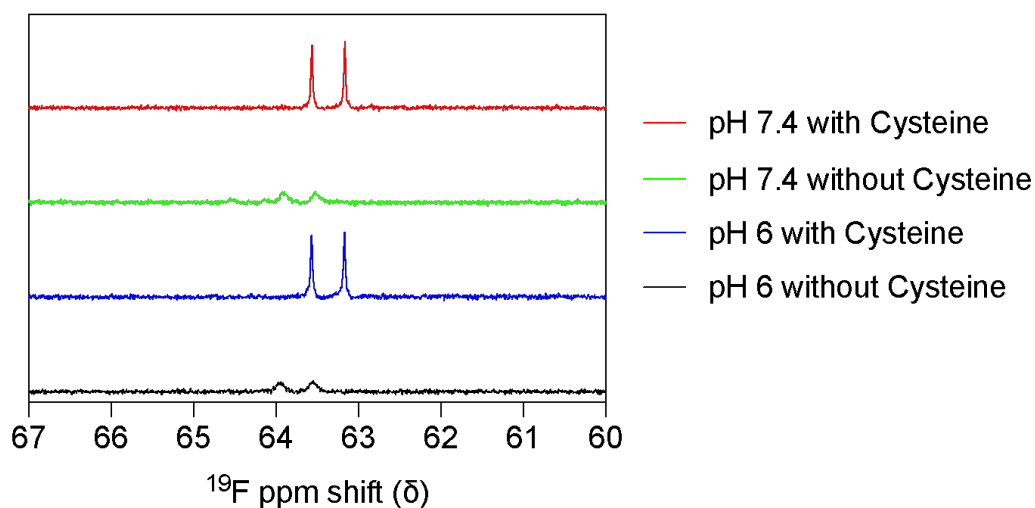


Figure S10 – ^{19}F NMR spectra of 1 mM $\text{Fe}^{\text{III}}\text{DO}_3\text{ASF}_5$ in deoxygenated 25 mM HEPES (pH 7.4), 50 mM KNO_3 and 25 mM MES (pH 6) with and without five equivalents cysteine. Each sample contains 20% DMSO and 20% D_2O . Spectra are zoomed in between +60 and +67 ppm to show broadened doublet. The quintet was not visible. All spectra were measured at least five minutes after preparation.

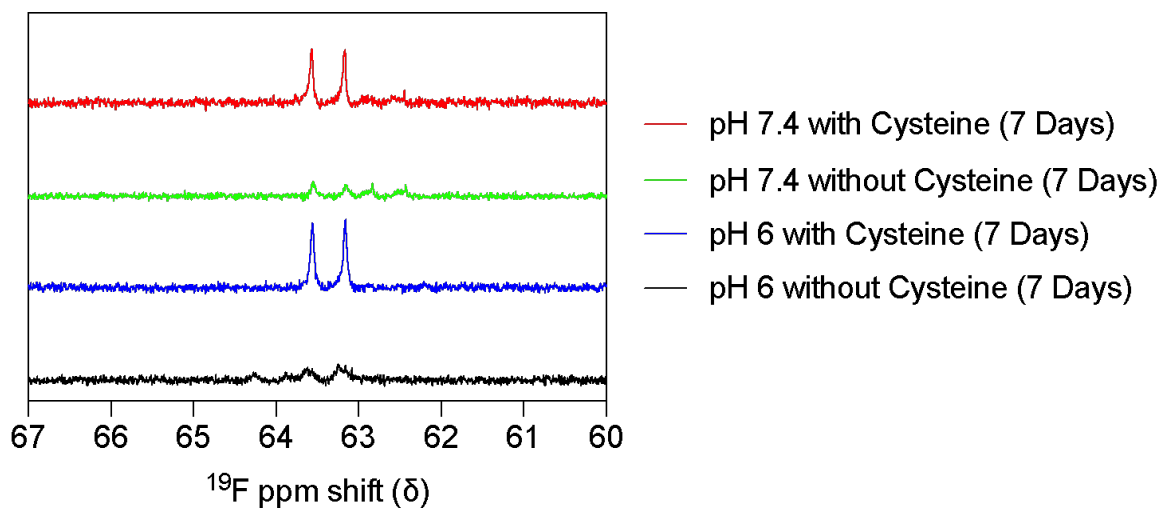


Figure S11 – ^{19}F NMR spectra of 1 mM $\text{Fe}^{\text{III}}\text{DO3ASF}_5$ in deoxygenated 25 mM HEPES (pH 7.4), 50 mM KNO_3 and 25 mM MES (pH 6) with and without five equivalents cysteine. Each sample contains 20% DMSO and 20% D_2O . Spectra are zoomed in between +60 and +67 ppm to show broadened doublet. The quintet was not visible. All spectra were measured seven days after preparation and no special precautions were made to protect samples from air beyond closing the cap and sealing with parafilm.

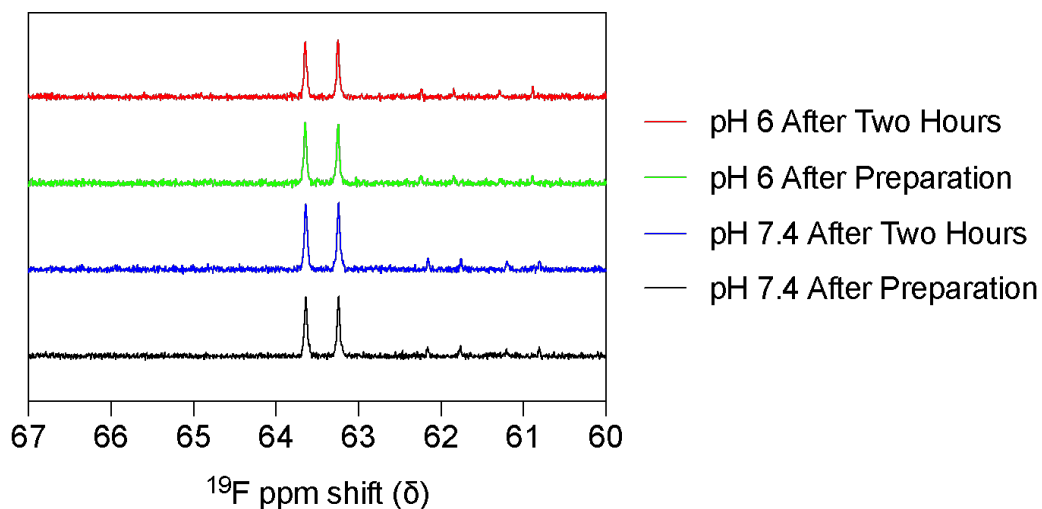


Figure S12 – ^{19}F NMR spectra of 1 mM $\text{Fe}^{\text{II}}\text{DO3ASF}_5$ in deoxygenated 5 mM HEPES (pH 7.4), 10 mM KNO_3 and 5 mM MES (pH 6) with 10% DMSO and 10% D_2O zoomed in between +60 and +67 ppm to show broadened doublet. The quintet was not visible. Samples were measured

directly after preparation (“After Preparation”) and two hours after preparation (“After Two Hours”).

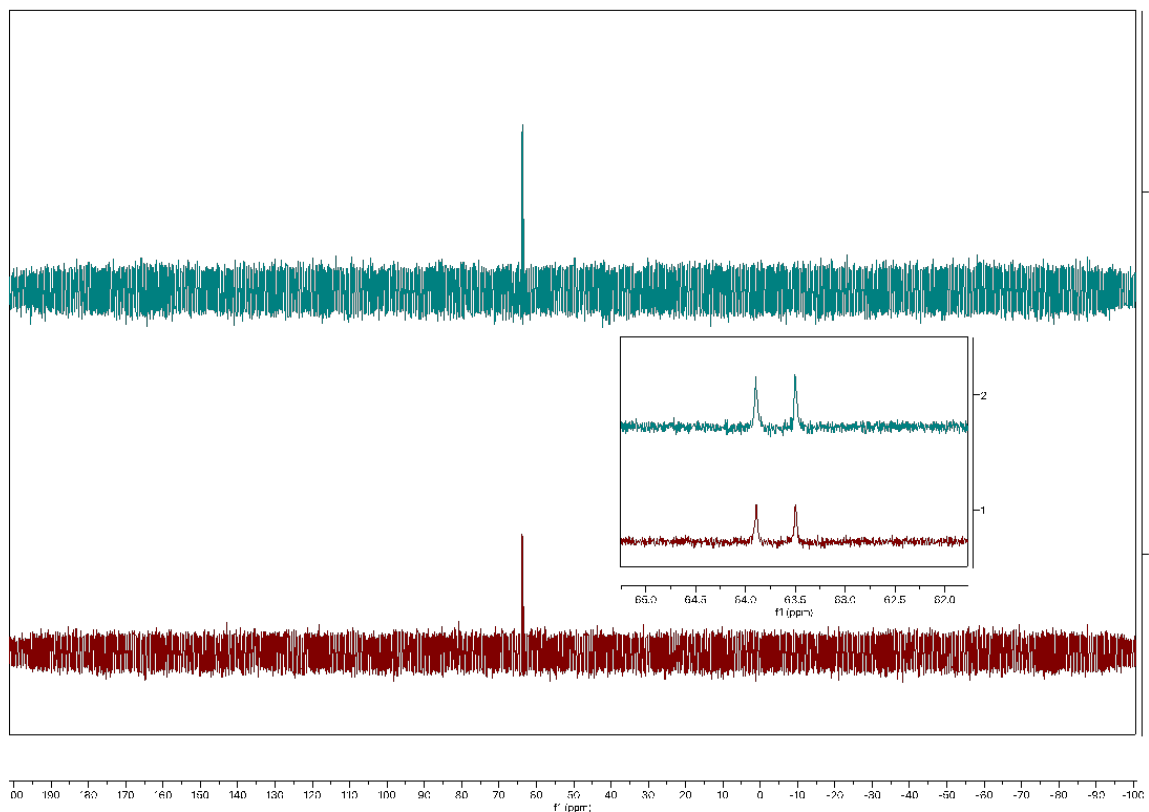


Figure S13 – Kinetic stability of $\text{Fe}^{\text{II}}\text{DO3ASF}_5$ in the presence of NaCl. ^{19}F NMR spectra of $\text{Fe}^{\text{II}}\text{DO3ASF}_5$ (1 mM) in the presence of 100 mM NaCl in 50 mM HEPES (pH 7.4). Before (bottom, red) or after (top, green) 24 h incubation at 37 °C. Inset shows a close-up of the ^{19}F peaks for $\text{Fe}^{\text{II}}\text{DO3ASF}_5$. 20% D_2O was added before the measurements for locking.

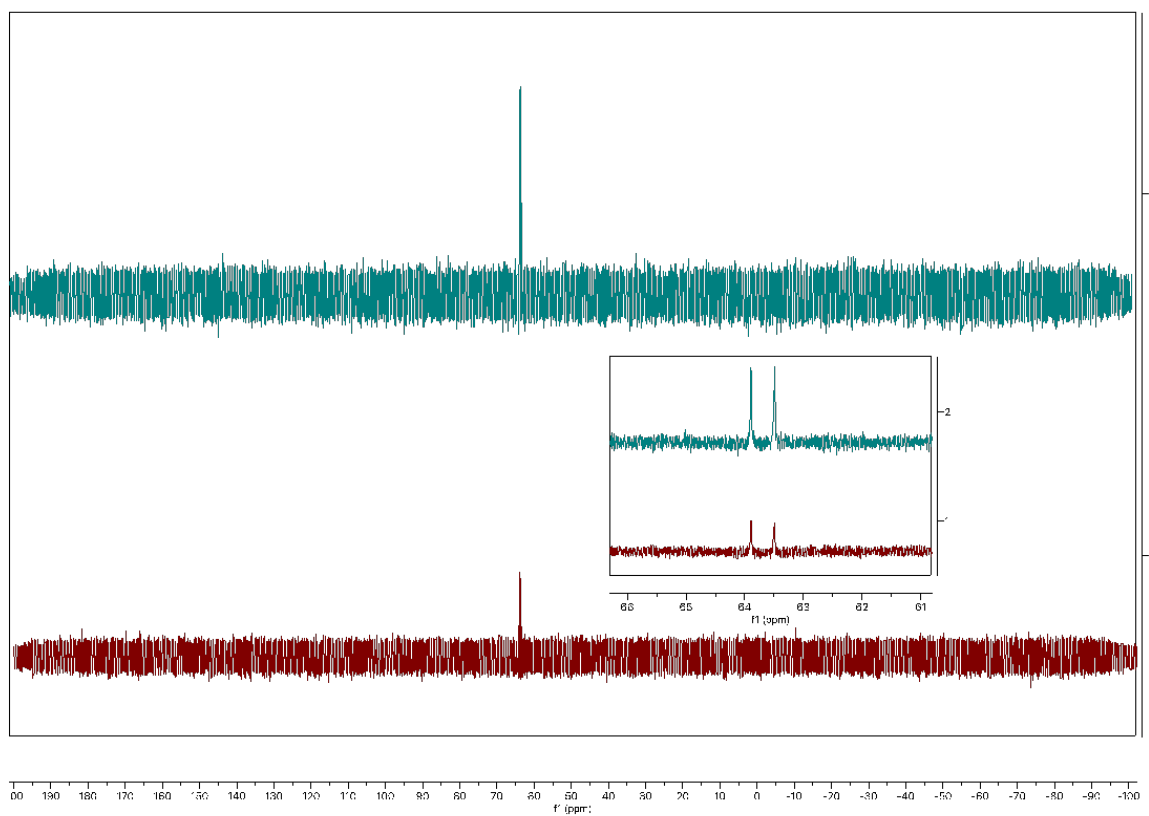


Figure S14 – Kinetic stability of $\text{Fe}^{\text{II}}\text{DO3ASF}_5$ in the presence of KCl. ^{19}F NMR spectra of $\text{Fe}^{\text{II}}\text{DO3ASF}_5$ (1 mM) in the presence of 100 mM KCl in 50 mM HEPES (pH 7.4). Before (bottom, red) or after (top, green) 24 h incubation at 37 °C. Inset shows a close-up of the ^{19}F peaks for $\text{Fe}^{\text{II}}\text{DO3ASF}_5$. 20% D_2O was added before the measurements for locking.

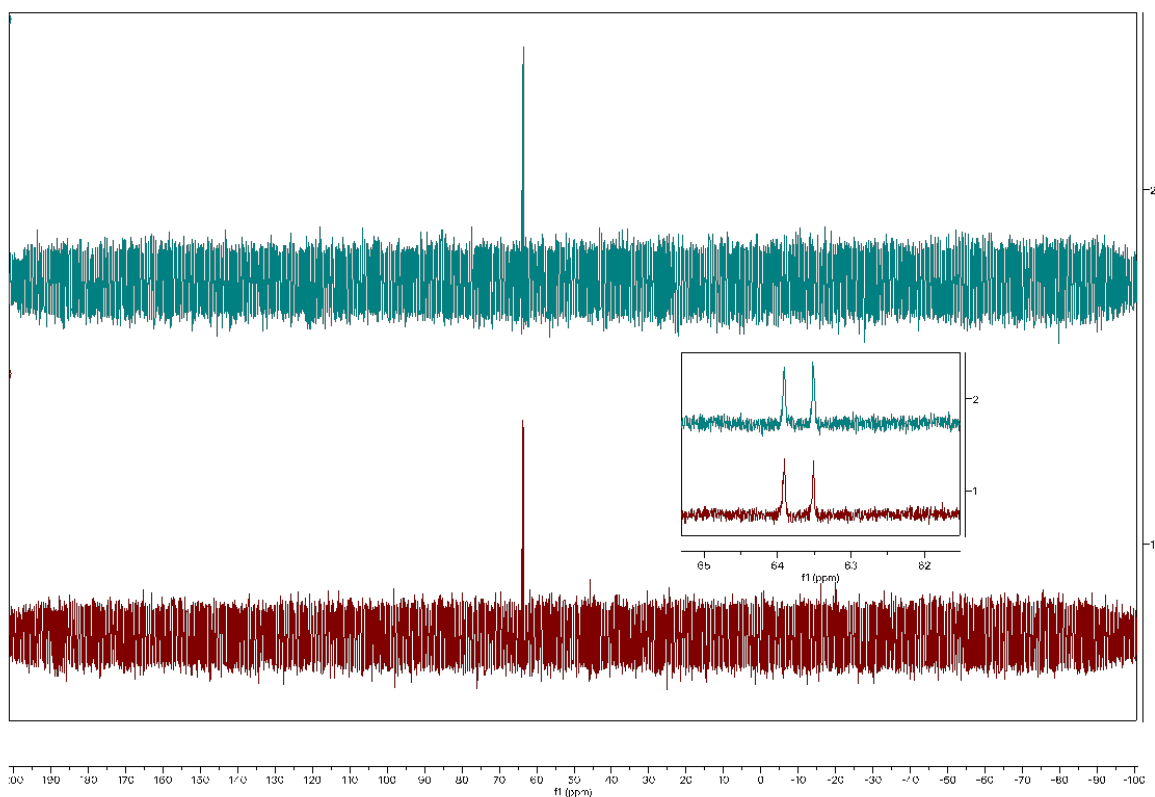


Figure S15 – Kinetic stability of $\text{Fe}^{\text{II}}\text{DO3ASF}_5$ in the presence of CaCl_2 . ^{19}F NMR spectra of $\text{Fe}^{\text{II}}\text{DO3ASF}_5$ (1 mM) in the presence of 10 mM CaCl_2 in 50 mM HEPES (pH 7.4). Before (bottom, red) or after (top, green) 24 h incubation at 37 °C. Inset shows a close-up of the ^{19}F peaks for $\text{Fe}^{\text{II}}\text{DO3ASF}_5$. 20% D_2O was added before the measurements for locking.

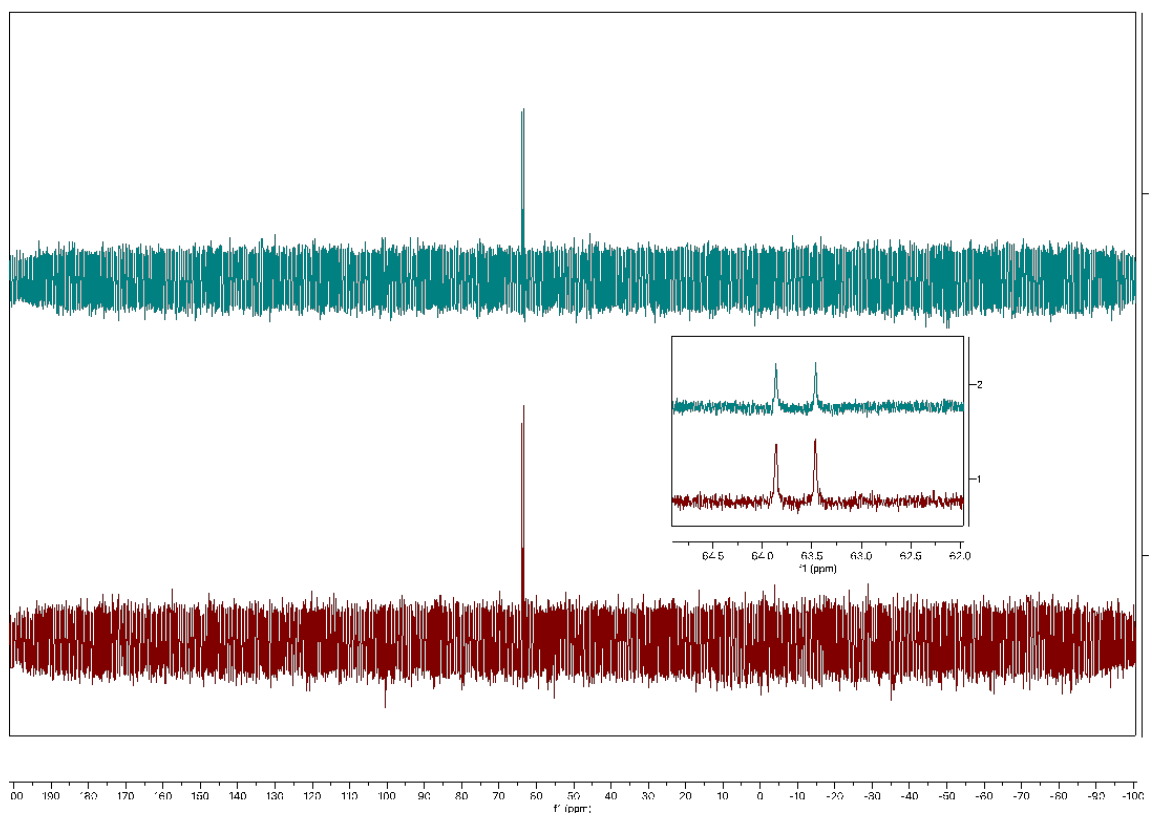


Figure S16 – Kinetic stability of $\text{Fe}^{\text{II}}\text{DO3ASF}_5$ in the presence of MgCl_2 . ^{19}F NMR spectra of $\text{Fe}^{\text{II}}\text{DO3ASF}_5$ (1 mM) in the presence of 10 mM MgCl_2 in 50 mM HEPES (pH 7.4). Before (bottom, red) or after (top, green) 24 h incubation at 37 °C. Inset shows a close-up of the ^{19}F peaks for $\text{Fe}^{\text{II}}\text{DO3ASF}_5$. 20% D_2O was added before the measurements for locking.

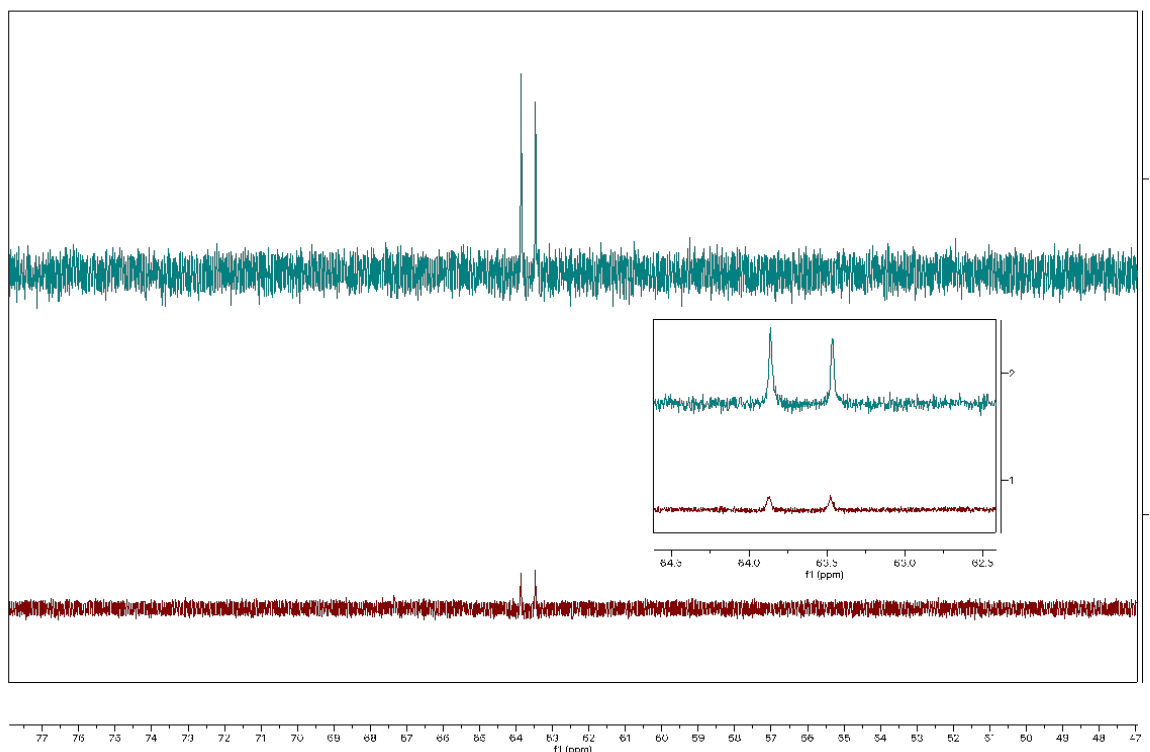


Figure S17 – Kinetic stability of $\text{Fe}^{\text{II}}\text{DO3ASF}_5$ in the presence of ZnCl_2 . ^{19}F NMR spectra of $\text{Fe}^{\text{II}}\text{DO3ASF}_5$ (1 mM) in the presence of 100 mM ZnCl_2 in 50 mM HEPES (pH 7.4). Before (bottom, red) or after (top, green) 24 h incubation at 37 °C. Inset shows a close-up of the ^{19}F peaks for $\text{Fe}^{\text{II}}\text{DO3ASF}_5$. 20% D_2O was added before the measurements for locking.

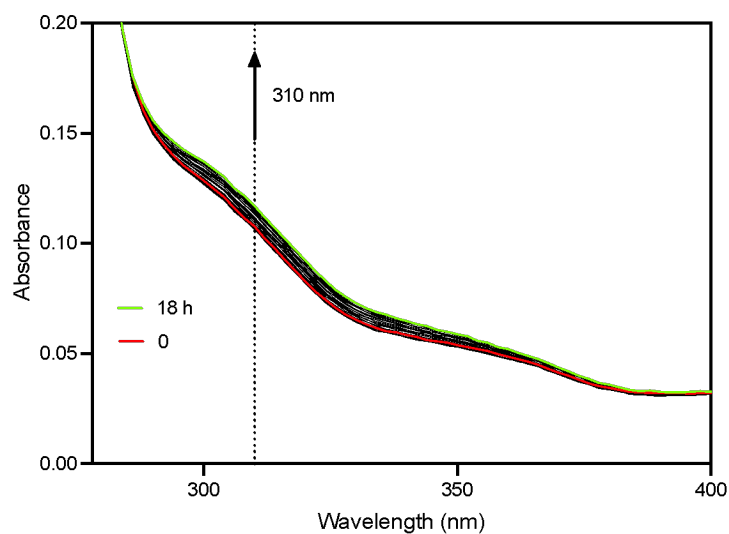


Figure S18 – Atmospheric oxidation of 100 μM $\text{Fe}^{\text{II}}\text{DO3ASF}_5$ in deoxygenated HEPES (pH 7.4) over (red) 0–18 h (green). Minimal oxidation was observed.

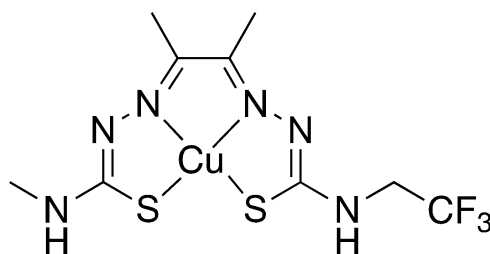


Figure S19 – Chemical structure of **CuATSM-F₃**.⁴

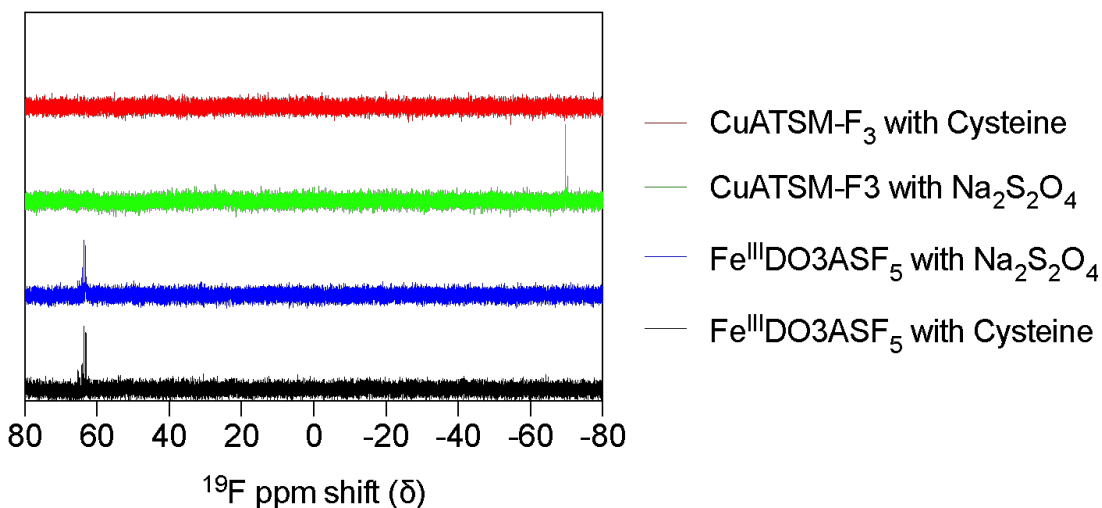


Figure S20 – ¹⁹F NMR spectra of 0.5 mM **CuATSM-F₃** with one equivalent cysteine (black),⁴ 0.5 mM **CuATSM-F₃** with one equivalent sodium dithionite (green), 0.5 mM **Fe^{III}DO3ASF₅** with one equivalent sodium dithionite, and 0.5 mM **Fe^{III}DO3ASF₅** with one equivalent cysteine. All samples were made in 3:2 d₆-DMSO:HEPES (5 mM pH 7.4) and all solvents were deoxygenated. No signal is shown for **CuATSM-F₃** with cysteine; however, a signal is shown for **CuATSM-F₃** with sodium dithionite (in the CF₃ region) and both **Fe^{III}DO3ASF₅** with cysteine and sodium dithionite (in the SF₅ region). Similarly, no signal is seen for the Fe complex in the CF₃ region as well as no signal is seen for the Cu complex in the SF₅ region.

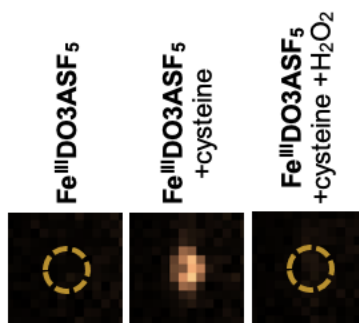


Figure S21 – ^{19}F MRI phantoms of 3 mM $\text{Fe}^{\text{III}}\text{DO3ASF}_5$ (left), 3 mM $\text{Fe}^{\text{III}}\text{DO3ASF}_5$ with one equivalent cysteine (middle), and 3 mM $\text{Fe}^{\text{III}}\text{DO3ASF}_5$ with one cysteine then 20 equivalents of H_2O_2 (right). All images were taken at the SF_5 frequency (282.588 MHz).

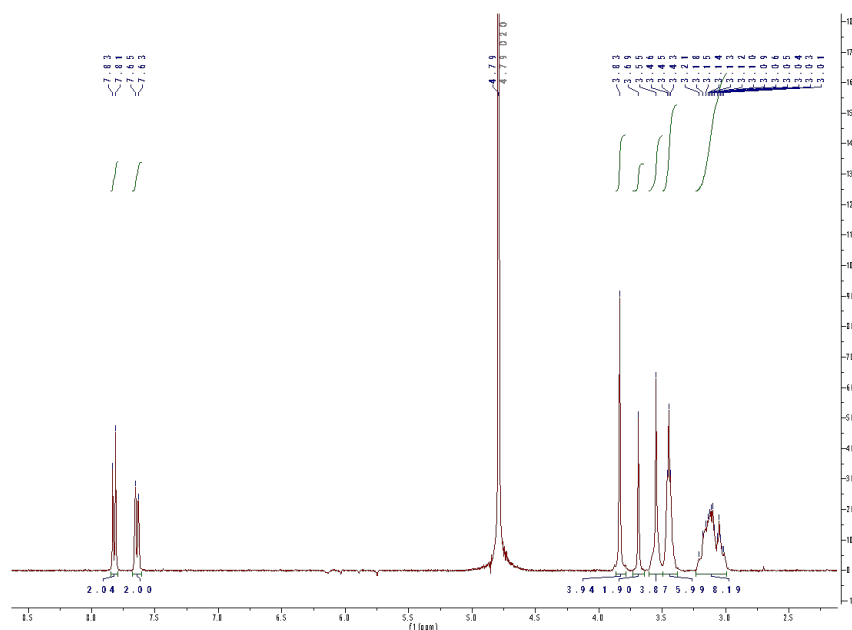


Figure S22 – ^1H NMR spectrum of DO3ASF_5 in D_2O at 25 °C.

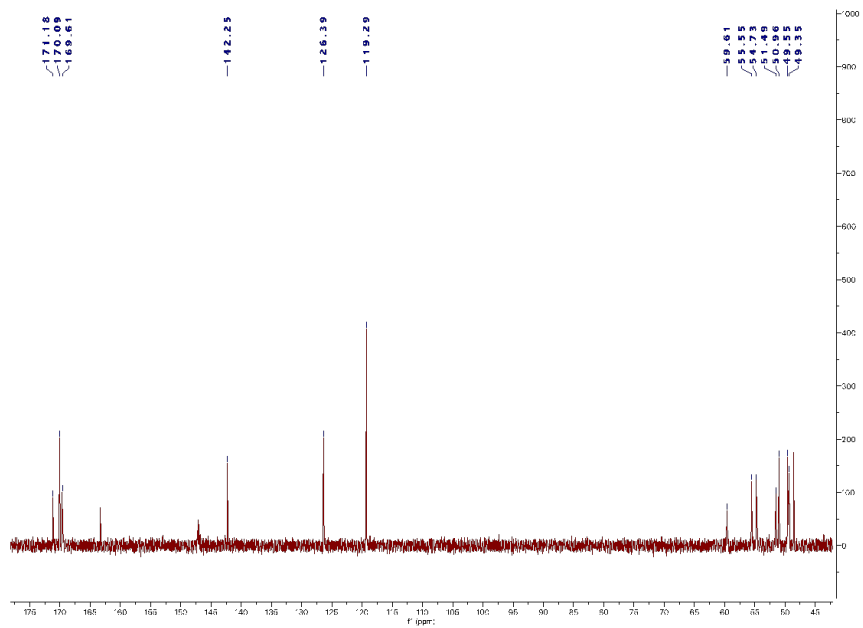


Figure S23 – ^{13}C NMR spectrum of **DO3ASF₅** in $\text{d}_6\text{-DMSO}$ at 25 °C. Spectrum shows peaks for MeOH (δ 48.59) and formic acid (δ 163.31).

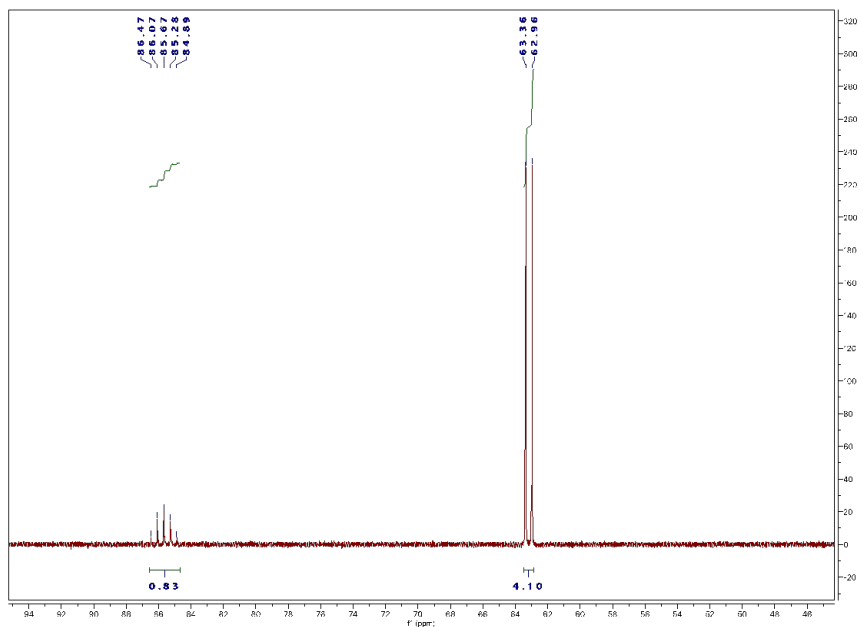


Figure S24 – ^{19}F NMR spectrum of **DO3ASF₅** in D_2O at 25 °C.

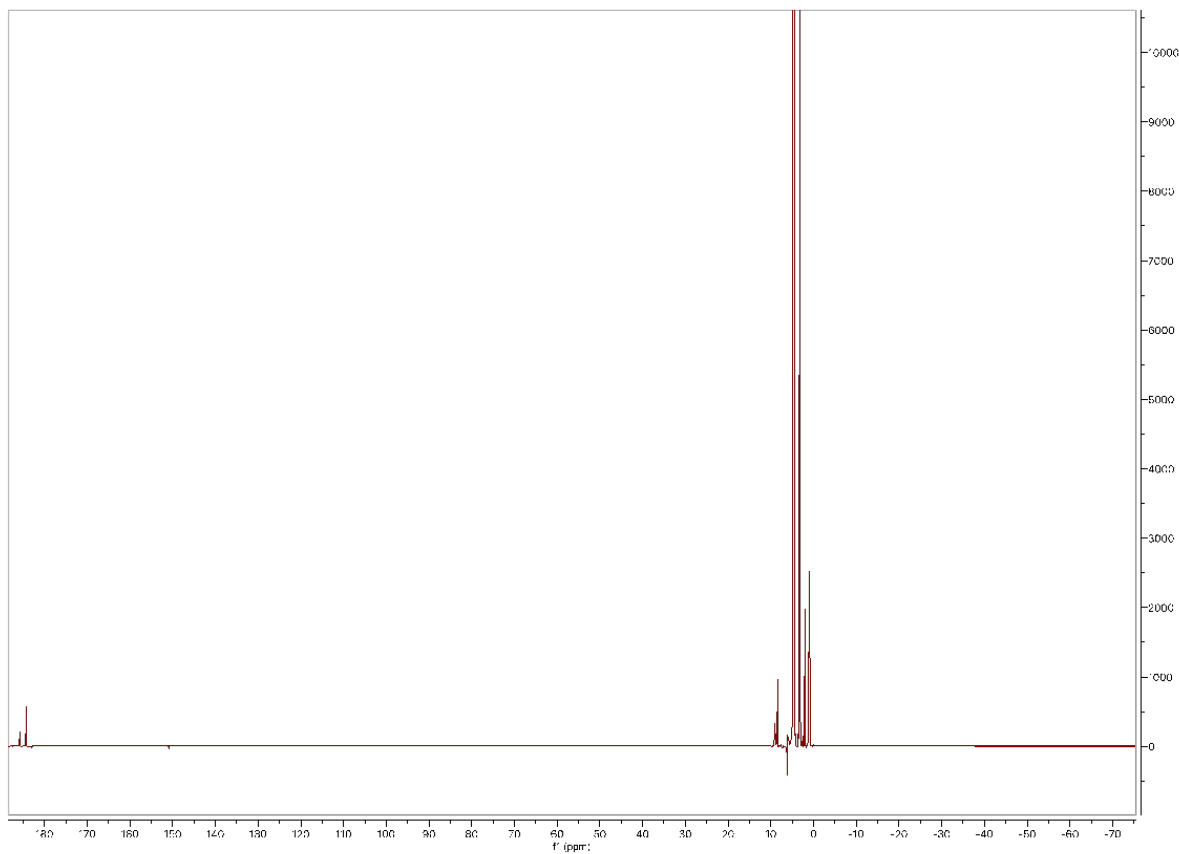
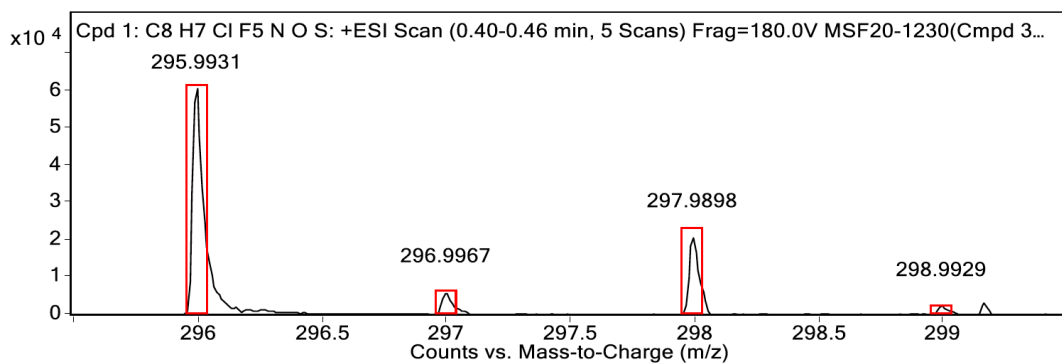


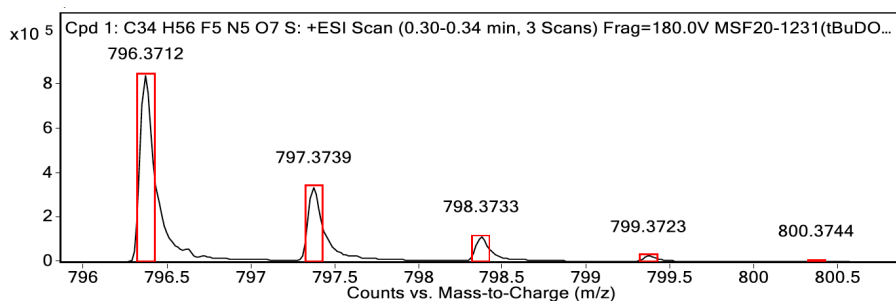
Figure S25 – ^1H NMR spectrum of $\text{Fe}^{\text{II}}\text{DO}_3\text{ASF}_5$ in D_2O



MS Spectrum Peak List

Obs. m/z	Calc. m/z	Charge	Abundance	Formula	Ion Species	Tgt Mass Error (ppm)
220.0219			332401			
295.9931	295.9930	1	61370	$\text{C}_8\text{H}_7\text{ClF}_5\text{NOS}$	$(\text{M}+\text{H})^+$	-0.47
296.9967	296.9958	1	6088	$\text{C}_8\text{H}_7\text{ClF}_5\text{NOS}$	$(\text{M}+\text{H})^+$	-2.95
297.9898	297.9900	1	20893	$\text{C}_8\text{H}_7\text{ClF}_5\text{NOS}$	$(\text{M}+\text{H})^+$	0.62
298.9929	298.9928	1	2389	$\text{C}_8\text{H}_7\text{ClF}_5\text{NOS}$	$(\text{M}+\text{H})^+$	-0.13
299.9884	299.9871	1	834	$\text{C}_8\text{H}_7\text{ClF}_5\text{NOS}$	$(\text{M}+\text{H})^+$	-4.11
300.9691	300.9897	1	162	$\text{C}_8\text{H}_7\text{ClF}_5\text{NOS}$	$(\text{M}+\text{H})^+$	68.42

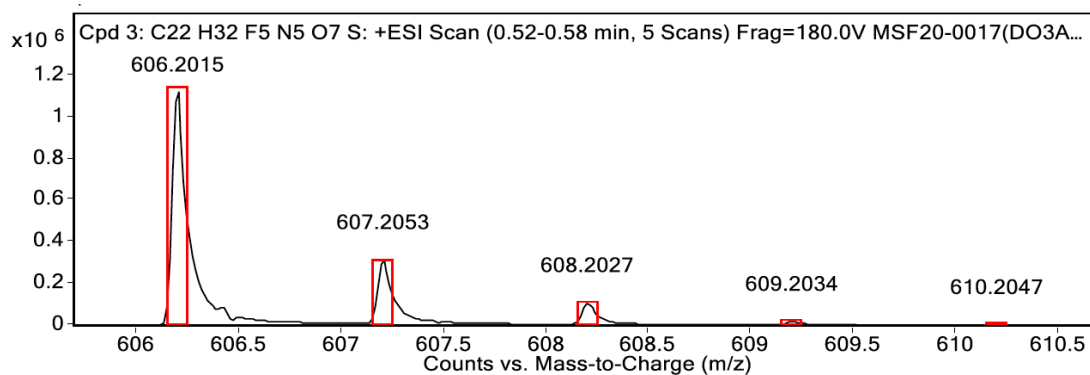
Figure S26 – FIA ESI^+ HRMS of $[\mathbf{3} + \text{H}]^+$. A small aliquot of the extracted EtOAc mixture was diluted to obtain the HRMS report above.



Obs. m/z	Calc. m/z	Charge	Abundance	Formula	Ion Species	Tgt Mass Error (ppm)
796.3712	796.3713	1	844613	C34H56F5N5O7S	(M+Na)+	0.09
797.3739	797.3743	1	338026	C34H56F5N5O7S	(M+Na)+	0.59
798.3733	798.3738	1	115427	C34H56F5N5O7S	(M+Na)+	0.67
799.3723	799.3747	1	25147	C34H56F5N5O7S	(M+Na)+	2.95
800.3744	800.3761	1	5068	C34H56F5N5O7S	(M+Na)+	2.04
801.3680	801.3778	1	792	C34H56F5N5O7S	(M+Na)+	12.17

--- End Of Report ---

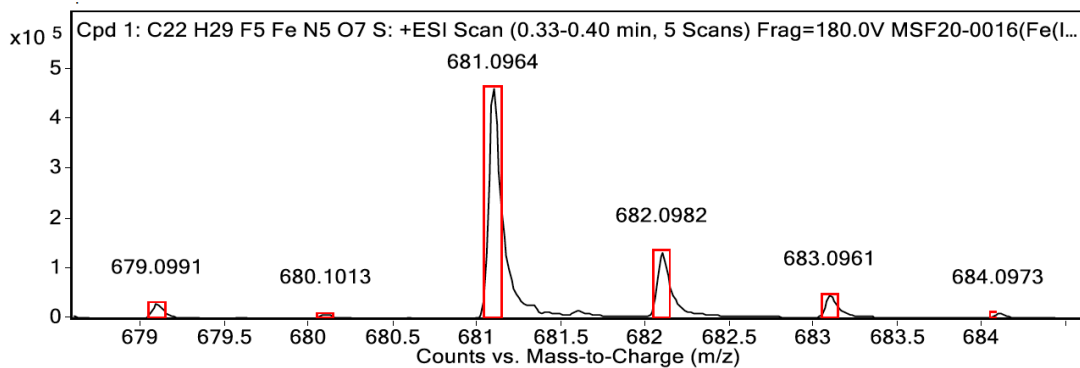
Figure S27 – FIA ESI⁺ HRMS of [^tBuDO₃ASF₅ + Na]⁺. A small aliquot of the DCM/MeOH mixture from the column was diluted to obtain the HRMS report above.



Obs. m/z	Calc. m/z	Charge	Abundance	Formula	Ion Species	Tgt Mass Error (ppm)
606.2015	606.2015	1	1130221	C22H32F5N5O7S	(M+H)+	0.06
607.2053	607.2044	1	314772	C22H32F5N5O7S	(M+H)+	-1.51
608.2027	608.2023	1	108767	C22H32F5N5O7S	(M+H)+	-0.66
609.2034	609.2036	1	18697	C22H32F5N5O7S	(M+H)+	0.39
610.2047	610.2048	1	3341	C22H32F5N5O7S	(M+H)+	0.17
644.1489			1282115			

--- End Of Report ---

Figure S28 – FIA ESI⁺ HRMS of [DO₃ASF₅ + H]⁺.

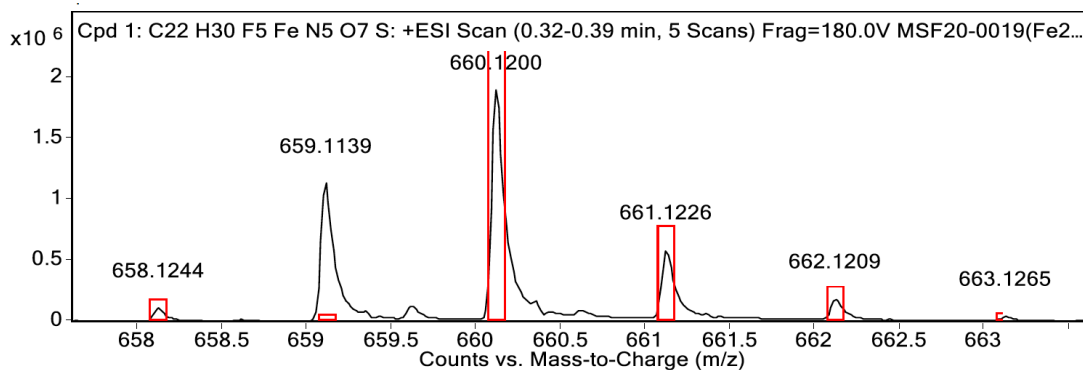


MS Spectrum Peak List

Obs. m/z	Calc. m/z	Charge	Abundance	Formula	Ion Species	Tgt Mass Error (ppm)
679.0991	679.0996	1	29488	C22H29F5FeN5O7S	(M+Na)+	0.75
680.1013	680.1025	1	9680	C22H29F5FeN5O7S	(M+Na)+	1.78
681.0964	681.0950	1	463955	C22H29F5FeN5O7S	(M+Na)+	-2.11
682.0982	682.0976	1	133265	C22H29F5FeN5O7S	(M+Na)+	-0.88
683.0961	683.0958	1	46462	C22H29F5FeN5O7S	(M+Na)+	-0.44
684.0973	684.0969	1	9187	C22H29F5FeN5O7S	(M+Na)+	-0.55
685.0938	685.0978	1	2216	C22H29F5FeN5O7S	(M+Na)+	5.83
686.0805	686.0992	1	2329	C22H29F5FeN5O7S	(M+Na)+	27.34
687.0779	687.1007	1	2154	C22H29F5FeN5O7S	(M+Na)+	33.16

--- End Of Report ---

Figure S29 – FIA ESI⁺ HRMS of [Fe^{III}DO3ASF₅ + Na]⁺.



MS Spectrum Peak List

Obs. m/z	Calc. m/z	Charge	Abundance	Formula	Ion Species	Tgt Mass Error (ppm)
658.1244	658.1255	1	110293	C22H30F5FeN5O7S	(M+H)+	1.68
659.1139	659.1284	1	1132222	C22H30F5FeN5O7S	(M+H)+	21.92
660.1200	660.1209	1	1908135	C22H30F5FeN5O7S	(M+H)+	1.38
661.1226	661.1235	1	586801	C22H30F5FeN5O7S	(M+H)+	1.44
662.1209	662.1217	1	185202	C22H30F5FeN5O7S	(M+H)+	1.26
663.1265	663.1228	1	41370	C22H30F5FeN5O7S	(M+H)+	-5.6
664.1273	664.1237	1	13091	C22H30F5FeN5O7S	(M+H)+	-5.38
665.1063	665.1251	1	6097	C22H30F5FeN5O7S	(M+H)+	28.3
666.1042	666.1266	1	2111	C22H30F5FeN5O7S	(M+H)+	33.6

--- End Of Report ---

Figure S30 – FIA ESI⁺ HRMS of [Fe^{II}DO3ASF₅ + H]⁺.

References

1. D. F. Evans, *J. Chem. Soc.*, 1959, 2003-2005.
2. P. B. Tsitovich, J. M. Cox, J. B. Benedict and J. R. Morrow, *Inorg. Chem.*, 2016, **55**, 700-716.
3. P. Srivastava, A. K. Tiwari, N. Chadha, K. Chuttani and A. K. Mishra, *Eur. J. Med. Chem.*, 2013, **65**, 12-20.
4. D. Xie, T. L. King, A. Banerjee, V. Kohli and E. L. Que, *J. Am. Chem. Soc.*, 2016, **138**, 2937-2940.